The Importance of Object-based Seed Sampling for Superpixel Segmentation

Felipe Belém*, Leonardo Melo*, Silvio Guimarães† and Alexandre Falcão*
*University of Campinas, Campinas-SP, 13083-852, Brazil
Email: felipedkstro@hotmail.com, leomelo168@gmail.com, afalcao@ic.unicamp.br
†Pontifical Catholic University of Minas Gerais, Belo Horizonte-MG, 31980-110, Brazil
Email: sjamil@pucminas.br

***Abstract*—Superpixel segmentation can be defined as an image partition into connected regions, such that image objects may be represented by the union of their superpixels.In this context, multiple iterations of superpixel segmentation from improved seed sets is a strategy exploited by several algorithms. The Iterative Spanning Forest (ISF) framework divides this strategy into three independent components: a seed sampling method, a superpixel delineation algorithm based on strength of connectedness between seeds and pixels, and a seed recomputation procedure. A recent work shows that object information can be added to each component of ISF such that the user can control the number of seeds inside the objects and so improve superpixel segmentation. However, it is uncertain how the added information impacts each component of the pipeline. Therefore, in this work, a study is conducted to evaluate such inclusion in the seed sampling procedure, partially elucidating its benefits. Additionally, we introduce a novel object-based sampling approach, named Object Saliency Map sampling by Ordered Extraction (OSMOX), and demonstrate the results for supervised and unsupervised object information. The experiments show considerable improvements in under-segmentation error, specially with a low number of superpixels.**

I. Introduction

Superpixel segmentation is the process of partitioning an image into connected regions of pixels that are similar according to some predicate (*e.g.,* color). The resulting superpixel-based image representation can improve efficiency and effectiveness of applications from many fields: (i) remote sensing [1]; (ii) pattern recognition [2]; and (iii) medical image analysis [3].

Algorithms for superpixel segmentation have been proposed and compared according to distinct measures [4]–[12]. Several algorithms adopt a three-stage pipeline based on seed pixels: (i) an initial seed sampling approach; (ii) a superpixel delineation method based on seed pixels; and (iii) a seed recomputation procedure. They update superpixel delineation in (ii) from refined seed sets from (iii) in order to improve effectiveness, as represented by boundary adherence and under-segmentation error. In this context, it is desirable that any object of interest can be precisely defined by the union of its superpixels. Ideally, a superpixel-based image representation should provide accurate object delineation with simple object representation (*i.e.*, minimum number of superpixels per object). However, the existing methods do not usually allow the user to control such a compromise between object delineation and representation.

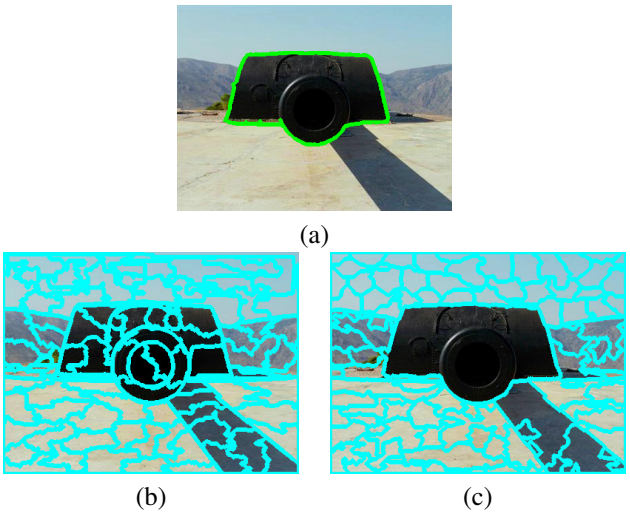

Fig. 1. (a) Image with the object's border in green. (b) state-of-the-art segmentation [10]; (c) our proposal. The number of desired superpixels was set to 100. Although both have a higher boundary adherence, clearly the latter offers the most suitable representation for object detection.

Authors in [13] propose a superpixel segmentation framework, named *Iterative Spanning Forest* (ISF), such that each stage of the aforementioned pipeline can be defined independently with no necessity to perform modifications in the remaining ones. To the best of our knowledge, this is the only framework with such flexibility. From a given set of seeds, ISF uses the *Image Foresting Transform* (IFT) algorithm [14] for superpixel delineation. The IFT defines superpixels by connecting each pixel to the seed which offers a path of lower cost to it on a given image graph, such that each superpixel is defined by a spanning tree composed by strongly connected pixels. Depending on the connectivity function (*i.e.*, path-cost function), the spanning trees are optimum path trees rooted at the seed pixels but the most effective results do not depend on the optimality of the forest [13]. Such flexibility has allowed the authors in [15] to add object information, as represented by an object saliency map [1], to each component of the ISF pipeline, providing user control over the number of superpixels per object.

[1]A map that assigns to each pixel a value proportional to its likelihood of belonging to a given object of interest.

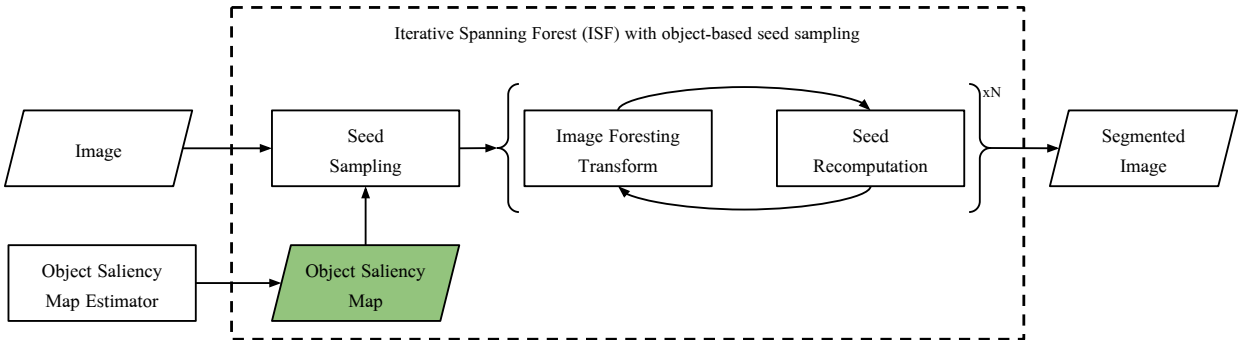

Fig. 2. Iterative Spanning Forest algorithm with the proposed modification (colored box) for the purpose of this work.

However, no study has been conducted to evaluate the importance of object information in each component of the ISF pipeline. In this work, we fulfill this gap with respect to the seed sampling strategy of ISF. It is worth mentioning that the understanding of such impact is beneficial to many applications. Figure 1 illustrates, for instance, how object-based seed sampling might impact the segmentation results and consequently object detection. We also propose a new seed sampling strategy, named *Object Saliency Map sampling by Ordered Extraction* (*OSMOX*) and evaluate ISF with object-based seed sampling on different types of object saliency maps: (i) supervised, (ii) unsupervised, and (iii) ideal. In (i), a classifier is trained from user-drawn markers in one image to estimate object saliency maps for the remaining images [16]. This is recommended when the object of interest appears in several images. In (ii), we use an object saliency algorithm suitable for natural images [17] and, in (iii), the gold standard segmentation is used as surrogate of a "perfect" saliency map. Thus, our contributions are two-fold: (i) a thorough study of how object-based seed sampling strategies impacts the segmentation results; and (ii) propose a novel object-based seed sampling approach.

In Section II, we present the state-of-the-art superpixel segmentation algorithms related to this work. In Section III, we describe the used methods for object saliency estimation and object-based seed sampling. The experimental setup and results are presented in Section IV. Finally, in Section V, we draw conclusions and discuss future work.

II. Related Works

Superpixel segmentation algorithms may minimize an energy function such that a graph partitioning problem is solved. In this graph, the pixels are the nodes and the arcs between pixels are weighted by a dissimilarity function. Superpixels are obtained by splitting (arc removal) the graph into parts [8], [10]. Among methods that follow this strategy, the *Entropy Rate Superpixel* (ERS) algorithm usually presents the best performance [10].

Another common strategy for superpixel segmentation is more closely related to the methods proposed in this work. These methods start from an initial seed set with the number of seeds equal to the number of desired superpixels. The dissimilarity between seeds and the remaining pixels is usually used to assign each pixel to the region of its most similar seed (as in a clustering approach based on the k-means algorithm). Each region is one superpixel and the seeds are recomputed to improve the seed set, repeating the process for a few iterations. Note that, this strategy cannot guarantee connected regions, except by some post-processing that might affect the number of desired superpixels. Examples are the popular *Simple Linear Iterative Clustering* (SLIC) [4], which can produce a fast superpixel segmentation, and its variants, such as the *Linear Spectral Clustering* (LSC) [7], the *Manifold SLIC* (MSLIC) [6], and the *Intrinsic MSLIC* (IMSLIC) [5].

Differently from the above clustering-based methods, but yet based on seeds, the *Iterative Spanning Forest* (ISF) framework [13] uses the dissimilarity between adjacent pixels as arc weights of an image graph to compute connectivity values between seeds and pixels. From an initial seed set, ISF uses the *Image Foresting Transform* (IFT) algorithm to obtain a spanning forest rooted at the seed set [14]. The seeds are recomputed to refine the results along multiple iterations of the IFT algorithm. The seeds compete among themselves such that each pixel is connected to the seed that reaches it with a path of cost lower than the cost offered by a previous seed. Each seed defines one connected superpixel as a spanning tree composed by strongly connected pixels. The superpixels are optimum-path trees depending on the connectivity function, but the most effective ISF-based methods do not require this condition [13]. In [15], the authors show the advantages of including object information in each component of ISF. Here, we evaluate the impact of object-based seed sampling in ISF-based superpixel segmentation using supervised and unsupervised methods for object saliency estimation (Figure 2). Therefore, we are focused on the first step of the pipeline. The methods for object-based seed sampling are described next.

III. Object-based Seed Sampling

In this section, we first describe supervised and unsupervised methods for *object saliency estimation*. We then describe two different object-based seed sampling strategies: the one proposed in [15] and a new approach.

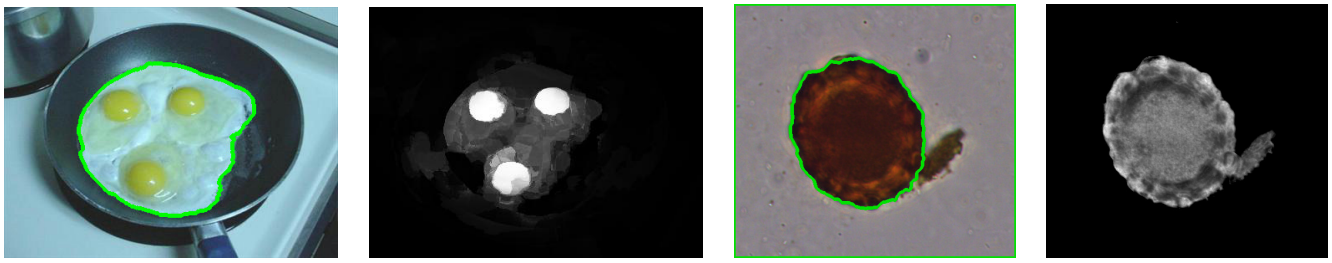

(a) (b) (c) (d)

Fig. 3. Examples of unsupervised and supervised object saliency estimation. (a) and (c) Image with the object's border in green. Object saliency maps as obtained based on (b) DSR for the image in (a), and (d) SUP for the image in (c).

A. Object Saliency Maps

Visual saliency is a property that makes objects stand out from their surroundings in images, capturing our attention. This property can be represented by an *object saliency map* — a map that assigns to each pixel its probability to be part of an object of interest. Object saliency maps are often seen as grayscale images, in which brighter pixels are those with higher saliency values. Moreover, such maps can be obtained through supervised or unsupervised learning algorithms.

In the context of unsupervised algorithms, the *Dense and Sparse Reconstruction* (DSR) [17], [18] is one of the state-of-the-art methods for natural images. It starts by performing a SLIC-based superpixel segmentation [4] and then estimates an object saliency map based on the dissimilarity between superpixels. It assumes that superpixels close to the center of the image are more likely to represent the object than superpixels connected to the image's border. Figure 3b illustrates the result of DSR for the natural image in Figure 3a.

In the context of supervised algorithms for applications where the object of interest appears in several images, the authors in [16] propose an object saliency map (hereafter denoted as SUP) that uses an IFT-based pixel classifier [19] as intermediate step. First, the user selects samples from the object and from the background, which will be divided into training and evaluation sets. Then, the method finds the most representative training samples such that a classifier is obtained based on one optimum-path forest rooted at representative object samples and one optimum-path forest rooted at representative background samples. An object saliency map is finally obtained by normalizing the minimum cost of a pixel to be conquered by the background roots using the sum of that cost from object and background roots. Figure 3d illustrates the result of SUP for the parasite image in Figure 3c. The classifier can then be applied to new images in which the object appears.

B. Object Geodesic Grid Sampling

For a given image with $\mathcal{I}$ pixels, a desired number N of seeds, and a desired percentage $p \in (0, 1)$ of seeds per object, the method *Object Geodesic Grid Sampling* (OGRID) aims to return a seed set $\mathcal{S}$ with pN object seeds and $(1-p)N$ background seeds [15]. For that, a threshold T at 50% of the maximum saliency value is applied to the object saliency map O by assuming that object pixels s have saliency values $O(s) \geq T$ and background pixels have values $O(s) < T$. The following algorithm is then applied separately to the foreground and background components that result from this thresholding operation.

The seeds are distributed per foreground component such that each component $c_i \subseteq \mathcal{I}, i = 1, \ldots, n$, should contain $N_i = \frac{pN|c_i|}{\sum_{i=1}^{n}|c_i|}$ seeds. Such a distribution favors large components (probable objects), whereas it assigns a few or no seeds to smaller components. The seeds per component c_i should also be separated by a distance $d > 0$ from each other. The algorithm uses two adjacent sets of a pixel s — $\mathcal{B}(s)$ is defined by a disk of radius d and center at s, and $\mathcal{B}^*(s)$ is defined as the border of that disk. Starting at a node $s \in c_i$, the algorithm inserts s to a seed set $\mathcal{S}_i$ and inserts the pixels in $\mathcal{B}^*(s)$ to a candidate seed set $\mathcal{C}$. While $|\mathcal{S}_i| < N_i$ and $\mathcal{C} \neq \emptyset$, the following steps are executed in order. A pixel t is removed from $\mathcal{C}$ and inserted to $\mathcal{S}_i$; every pixel $u \in \mathcal{B}^*(t)$ is inserted to $\mathcal{C}$; and every pixel $u \in \bigcup_{s \in \mathcal{S}_i} \mathcal{B}(s) \setminus \mathcal{B}^*(s)$ is removed from $\mathcal{C}$. At the end, $\mathcal{S} \leftarrow \mathcal{S} \cup \mathcal{S}_i$, $i = 1, 2, \ldots, n$. Similarly, it works for the background components. However, the minimum distance d between seeds inside each component might result $\mathcal{S}$ with $|\mathcal{S}| < N$. We then optimize d such that the number of sampled seeds in each c_i better approximates N_i.

In order to avoid the parameter T, fix d as a function of $\mathcal{I}$, p, and N, but not using it as a constraint, and make $|\mathcal{S}| = N$, we propose the seed sampling approach presented next.

C. Object Saliency Map Sampling By Ordered Extraction

In *Object Saliency Map Sampling By Ordered Extraction* (OSMOX), by considering a percentage p of object seeds, we first fix $d = \sqrt{\frac{|\mathcal{I}|}{Np}}$ for foreground seed estimation and $d = \sqrt{\frac{|\mathcal{I}|}{N(1-p)}}$ for background seed estimation, by following the idea of grid seed sampling from [4]. Similarly to OGRID, an adjacent set $\mathcal{B}(s)$ is defined with radius d and center at s. For speeding purposes, let $\mathcal{C}(s) \subseteq \mathcal{B}(s)$ in which the distance of s to any adjacent pixel is no more than $\sqrt{d}$. Thus, the priority value $P(s)$ of a pixel s be selected as seed is a function of the object saliency map O, defined as $P(s) = \sum_{\forall t \in \mathcal{C}(s)} O(t)$. Using a priority queue Q, each pixel

(a) (b) (c) (d)

Fig. 4. Examples of seed sampling using each object-based approach. (a) and (c) OGRID. (b) and (d) OSMOX. Both considering the saliency maps in Figure 3, with $N = 20$ and $p = 0.9$. Note that OGRID is unable to select the number N of desired seeds.

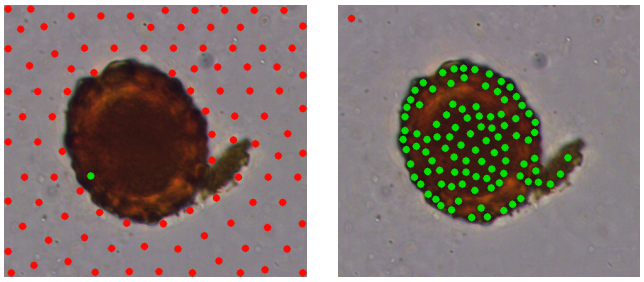

(a) (b)

Fig. 5. OSMOX using different percentages of object seeds for $N = 100$. (a) $p = 0.01$ and (b) $p = 0.99$. In both cases, it can guarantee the desired ratio between the numbers of object and background seeds.

$s \in \mathcal{I}$ is inserted to Q with priority $P(s)$. A first pixel s with the highest priority is removed from Q and inserted to the seed set $\mathcal{S}$. At this moment, all pixels $t \in \mathcal{B}(s)$ have their priority values reduced by $P(t) \leftarrow (1 - \exp \frac{-\|s,t\|^2}{2\sigma^2})P(t)$ and their position in the priority queue updated accordingly. For a suitable dispersion of the seeds, we recommend $\sigma = \frac{d}{0.6}$. The removal of a next seed pixel from Q and the priority reduction process are repeated until the desired number of seeds is reached or $Q = \emptyset$. Similarly, this algorithm is applied to the complement of O for background seed selection.

Figure 4 illustrates the sampling behaviors of OGRID and OSMOX, considering unsupervised and supervised object saliency maps. OGRID selects seeds within components of higher saliency values, while OSMOX also selects seeds in regions of less confidence in the map. Additionally, OSMOX guarantees the number N of desired seeds. For a suitable object saliency map and by choice of p, OSMOX allows better user control over the proportion of seeds inside and outside the object (Figure 5).

Regarding the execution time, GRID outperforms both object-based approaches due to the absence of pre-processing steps. Comparing OSMOX and OGRID, the former is not affected by the number of connected salient regions, while OGRID excels in unusual situations — large images, with a few small salient objects. On average, the speed-up achieved by GRID over OSMOX ranges from 65 to 13, whereas OSMOX over OGRID ranges from 6 to 2, when the amount of superpixels varies in $[10, 1000]$.

IV. Experimental Results

In this section, we describe our experimental setup, such as parameter selection, datasets, and evaluation metrics. Then, we present the results obtained when considering a supervised, an unsupervised, and an ideal object saliency map through quantitative and qualitative analysis.

A. Experimental Setup

The experiments use three datasets as follows. *MSRA1K* [20] is a dataset with natural images and a single unambiguously-salient object per image. *Birds* [21] is a dataset of natural images of birds — objects with thin and elongated parts. Both datasets are suitable to use DSR for unsupervised object saliency estimation. We also use *Parasites* [15] — a dataset suitable for supervised object saliency estimation. This dataset contains optical microscopy images of human intestinal parasites.

For comparison, we adopt the regular grid seed sampling (GRID) and the following baselines: (i) ERS [10] — the most competitive method in MSRA1K; (ii) LSC [7]; (iii) SLIC [4]; and (iv) ISF-GRID-ROOT [13] (ISF-GRID, for simplicity) — the most competitive method in Birds. The ISF variants based on OGRID and OSMOX are denoted as ISF-OGRID and ISF-OSMOX, respectively. In Parasites, it was not possible to perform the segmentation using the ERS algorithm, since its implementation (available online) considers only 8-bit images (the parasite images have 16 bits).

The methods are evaluated by the popular measures *Boundary Recall* (BR) [4] and *Under-segmentation Error* (UE) [22] in an interval from 10 to 100 superpixels. BR measures the adherence of the borders of the superpixels to the object's border. UE detects when a superpixel mostly inside the object contains background pixels and when a superpixel mostly inside the background contains object pixels. Thus, we aim higher BR and lower UE.

In all experiments, the parameters of the baselines are fixed as suggested in their original works. In ISF-OGRID and ISF-OSMOX, we also fix the parameters of the ISF algorithm. The remaining parameter p (percentage of object seeds) is then optimized based on BR and UE for OGRID and OSMOX, as shown in Table I where D_1 is Birds, D_2 is MSRA1K, and D_3

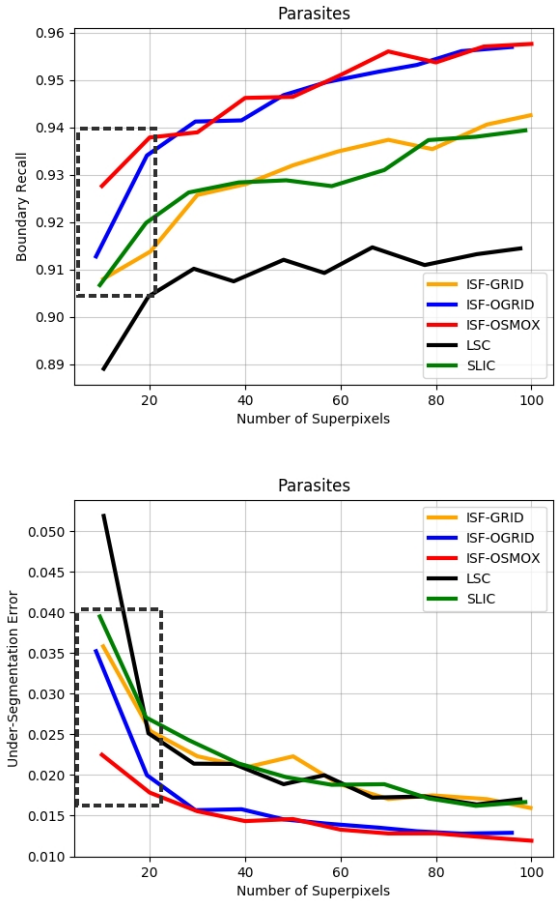

Fig. 6. Results obtained in Parasites dataset for BR and UE, respectively, by using the SUP object saliency estimator.

is Parasites. For this optimization, we use 10% of each dataset. Therefore, the tests are executed on the remaining 90% of each dataset.

Method	DSR		SUP	GT		
	D_1	D_2	D_3	D_1	D_2	D_3
ISF-OGRID	0.3	0.9	0.9	0.8	0.9	0.9
ISF-OSMOX	0.7	0.9	0.9	0.7	0.9	0.6

TABLE I
OBJECT PERCENTAGE PARAMETER p FOR OGRID AND OSMOX ON EACH DATASET, WHERE D_1 IS BIRDS, D_2 IS MSRA1K, AND D_3 IS PARASITES.

B. Experiments using Supervised Saliency Maps

In Parasites, we use the SUP saliency estimator to show that both object-based seed sampling strategies outperform the baselines due to the quality of the object saliency map (Figure 6). For higher number of superpixels, ISF-OGRID and ISF-OSMOX tend to be equivalent. For lower number of superpixels, ISF-OSMOX can significantly outperform ISF-OGRID since it approximates better the number of desired seeds. Moreover, the number of objects of interest per image is never greater than 5 in Parasites. Therefore, we are mostly interested in a few superpixels (as depicted by a dashed rectangle in the charts). This conclusion is also valid for both BR and UE.

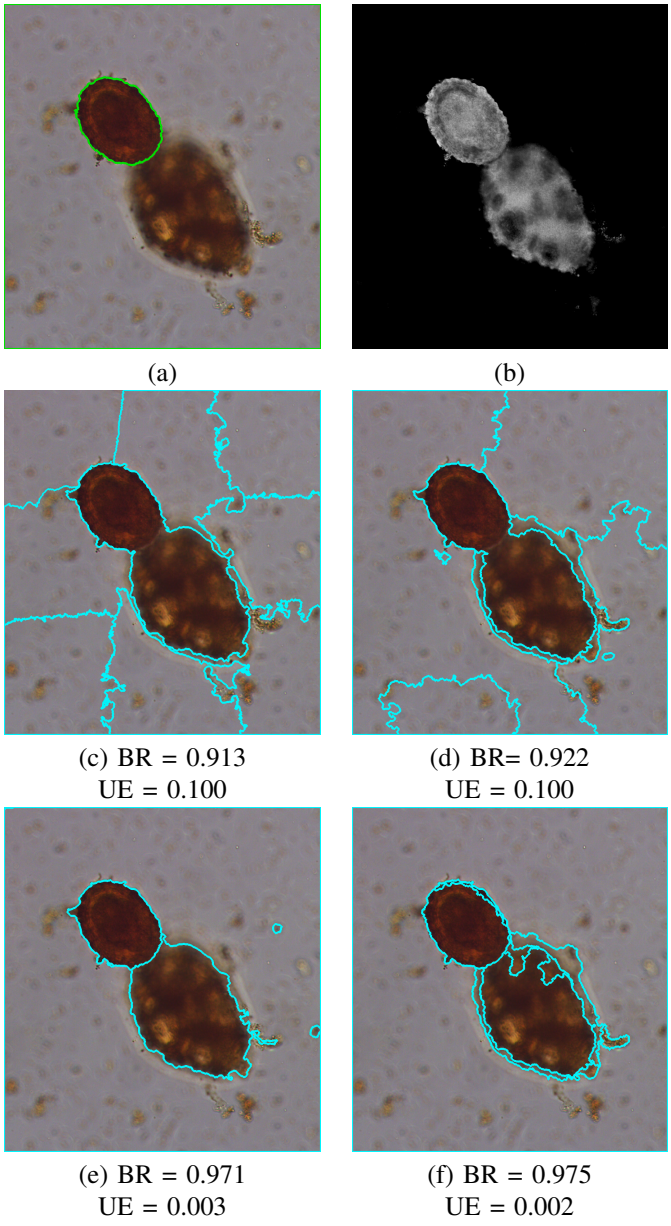

Fig. 7. (a) Image with the object's border in green. (b) Object saliency map by SUP. Segmentation with $N = 10$ by (c) SLIC, (d) ISF-GRID, (e) ISF-OGRID, and (f) ISF-OSMOX. For OGRID and OSMOX, $p = 0.9$ (Table I) on the map (b).

Figure 7 illustrate a qualitative comparison among the methods. Although SLIC and ISF-GRID present good delineation and representation of the object, both ISF-OGRID and ISF-OSMOX can better separate the parasite egg from the impurity. When comparing ISF-OGRID and ISF-OSMOX, it is worth noticing that ISF-OSMOX is the only one that guarantees the exact number of desired superpixels.

C. Experiments using Unsupervised Saliency Maps

Figure 8 presents the BR and UE curves of the methods for Birds and MSRA1K, using DSR for unsupervised object

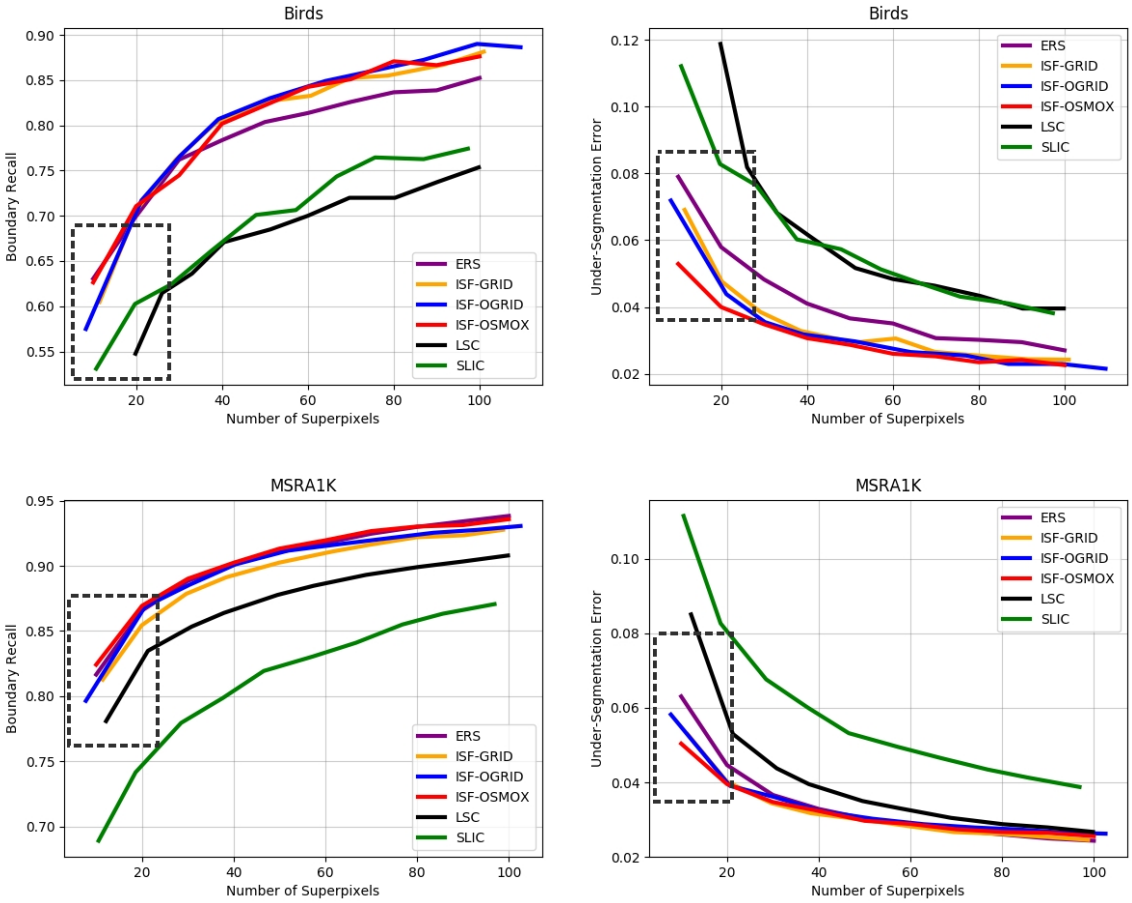

Fig. 8. Results obtained in Birds and MSRA1K for BR and UE, respectively, and using DSR as object saliency estimator.

saliency estimation. In this case, the quality of the saliency map is lower, but ISF-OGRID and ISF-OSMOX are able to achieve similar good performance to the most competitive baselines for each dataset: ERS in MSRA1K and ISF-GRID in Birds. Indeed for lower number of superpixels (dashed rectangle), the proposed methods provide better UE than these baselines, being ISF-OSMOX the best approach. Similar to Parasites, the images in both datasets do not contain more than 10 objects of interest.

Figures 9 and 10 present a qualitative comparison between ERS and the ISF-based methods. ISF-based methods present good delineation performance, but the best results are clearly obtained by those that use object-based seed sampling. Moreover, ISF-OSMOX shows good results on both, boundary adherence and under-segmentation error.

D. Experiments using Ideal Saliency Maps

Figure 11 shows the BR and UE curves for the ISF-based approaches with object-based seed sampling on the three datasets and using DSR and GT (the "ideal" object saliency map, as represented by the gold standard segmentations). One can see that ISF-OGRID and ISF-OSMOX using GT present a significant improvement as compared to their versions with DSR. This is a clear indication that improvements in unsupervised object saliency estimation can positively affect those ISF-based methods. In Parasites, on the other hand, since SUP already provides a good object saliency map, the use of GT does not improve the results of ISF-OGRID and ISF-OSMOX. In this case, the uncertainties of the saliency map have a positive influence on the seed sampling approaches.

V. Conclusion

We have evaluated the impact of object-based seed sampling methods in ISF-based superpixel segmentation algorithms. In this context, we presented two approaches, ISF-OGRID and ISF-OSMOX, being the latter a relevant contribution for the case of a low number of superpixels.

Our findings show that the inclusion of object information in the initial seed sampling strategy can significantly improve the segmentation results, specially the under-segmentation error. Moreover, possible improvements in unsupervised object saliency estimation can positively affect the performance of ISF-OGRID and ISF-OSMOX, being this a subject for future investigation.

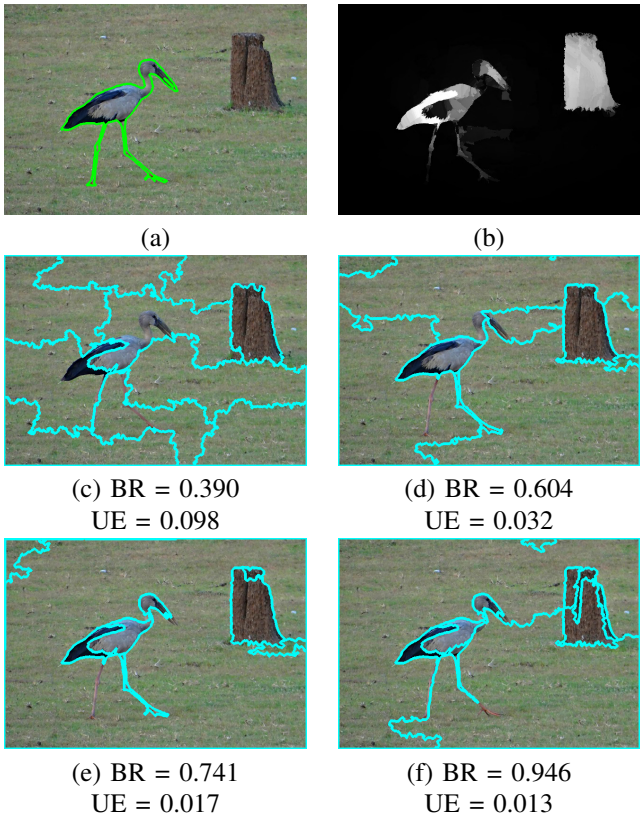

(a) (b) (c) BR = 0.390 UE = 0.098 (d) BR = 0.604 UE = 0.032 (e) BR = 0.741 UE = 0.017 (f) BR = 0.946 UE = 0.013

Fig. 9. (a) Image with the object's border in green. (b) Object saliency map by DSR. Segmentation with $N = 10$ by (c) ERS, (d) ISF-GRID, (e) ISF-OGRID, and (f) ISF-OSMOX. For OGRID and OSMOX, $p = 0.3$ and $p = 0.7$ (Table I), respectively, on the map (b).

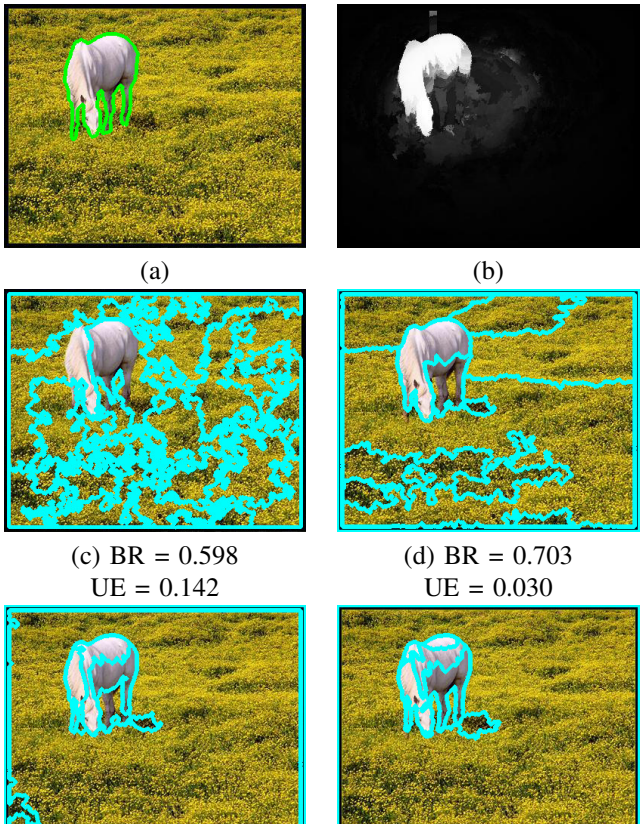

(a) (b) (c) BR = 0.598 UE = 0.142 (d) BR = 0.703 UE = 0.030 (e) BR = 0.801 UE = 0.023 (f) BR = 0.941 UE = 0.012

Fig. 10. (a) Image with the object's border in green. (b) Object saliency map by DSR. Segmentation with $N = 10$ by (c) ERS, (d) ISF-GRID, (e) ISF-OGRID, and (f) ISF-OSMOX. For OGRID and OSMOX, $p = 0.9$ (Table I) on the map (b).

ACKNOWLEDGEMENTS

This study was financed in part by the Coordenação de Aperfeiçoamento de Pessoal de Nível Superior - Brasil (CAPES COFECUB 88887.191730/2018-00), CNPq (302970/2014-2, 421521/2016-3, 307062/2016-3, 131000/2018-7, 134659/2018-0, 303808/2018-7), FAPEMIG/PPM (6-16), and by FAPESP (2014/12236-1).

REFERENCES

[1] H. He, J. Zhou, M. Chen, T. Chen, D. Li, and P. Cheng, "Building extraction from uav images jointly using 6d-slic and multiscale siamese convolutional networks," Remote Sensing, vol. 11, no. 9, p. 1040, 2019.

[2] S. Zhang, H. Wang, W. Huang, and Z. You, "Plant diseased leaf segmentation and recognition by fusion of superpixel, k-means and phog," Optik, vol. 157, pp. 866–872, 2018.

[3] Y. Li and L. Shen, "Skin lesion analysis towards melanoma detection using deep learning network," Sensors, vol. 18, no. 2, p. 556, 2018.

[4] R. Achanta, A. Shaji, K. Smith, A. Lucchi, P. Fua, and S. Süsstrunk, "SLIC superpixels compared to state-of-the-art superpixel methods," IEEE Trans. Pattern Anal. Mach. Intell., vol. 34, pp. 2274–2282, 2012.

[5] Y.-J. Liu, M. Yu, B.-J. Li, and Y. He, "Intrinsic manifold SLIC: A simple and efficient method for computing content-sensitive superpixels," IEEE Trans. Pattern Anal. Mach. Intell., vol. 40, no. 3, pp. 653–666, March 2018.

[6] Y.-J. Liu, C.-C. Yu, M.-J. Yu, and Y. He, "Manifold SLIC: A fast method to compute content-sensitive superpixels," in Proc. 29th Conf. Comput. Vis. Pattern Recognit., 2016, pp. 651–659.

[7] Z. Li and J. Chen, "Superpixel segmentation using linear spectral clustering," in Proc. 28th Conf. Comput. Vis. Pattern Recognit., June 2015, pp. 1356–1363.

[8] J. Shi and J. Malik, "Normalized cuts and image segmentation," IEEE Trans. Pattern Anal. Mach. Intell., vol. 22, pp. 888–905, 2000.

[9] P. Felzenszwalb and D. Huttenlocher, "Efficient graph-based image segmentation," Intl. Journal Comput. Vis., vol. 59, no. 2, pp. 167–181, 2004.

[10] M.-Y. Liu, O. Tuzel, S. Ramalingam, and R. Chellappa, "Entropy rate superpixel segmentation," in IEEE 24th Conf. Comput. Vis. Pattern Recognit. (CVPR). IEEE, 2011, pp. 2097–2104.

[11] O. Veksler, Y. Boykov, and P. Mehrani, "Superpixels and supervoxels in an energy optimization framework," in 11th European Conf. Comput. Vis. (ECCV). Springer, 2010, pp. 211–224.

[12] A. Rubio, L. Yu, E. Simo-Serra, and F. Moreno-Noguer, "Bass: boundary-aware superpixel segmentation," in IEEE 23rd Intl. Conf. Pattern Recognit. (ICPR). IEEE, 2016, pp. 2824–2829.

[13] J. E. Vargas-Muñoz, A. S. Chowdhury, E. B. Alexandre, F. L. Galvão, P. A. V. Miranda, and A. X. Falcão, "An iterative spanning forest framework for superpixel segmentation," IEEE Trans. Image Process., 2019, to appear.

[14] A. X. Falcão, J. Stolfi, and R. A. Lotufo, "The image foresting transform: Theory, algorithms, and applications," IEEE Trans. Pattern Anal. Mach. Intell., vol. 26, pp. 19–29, 2004.

[15] F. Belém, S. Guimarães, and A. Falcão, Superpixel Segmentation by Object-Based Iterative Spanning Forest: 23rd Iberoamerican Congress, CIARP 2018, Madrid, Spain, November 19-22, 2018, Proceedings. Elsevier, 2019, pp. 334–341.

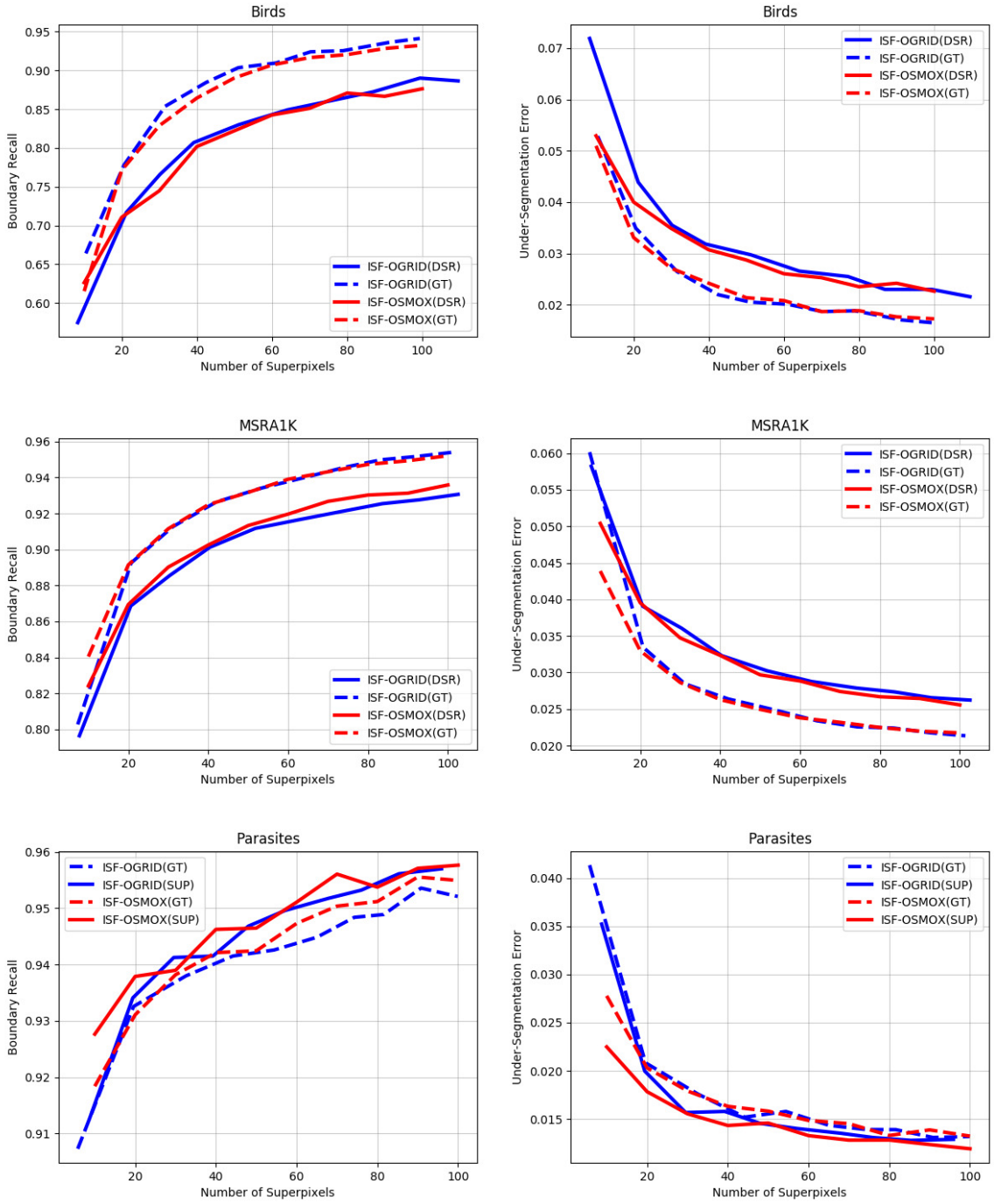

Fig. 11. Results obtained in Birds, MSRA1K, and Parasites for BR and UE, respectively, using DSR, SUP, and GT estimators depending on the case.

[16] T. V. Spina and A. X. Falcão, "Intelligent understanding of user input applied to arc-weight estimation for graph-based foreground segmentation," in Proc. 23th Conf. Graphics Pattern Images (SIBGRAPI), 2010, pp. 164–171.

[17] X. Li, H. Lu, L. Zhang, X. Ruan, and M.-H. Yang, "Saliency detection via dense and sparse reconstruction," in IEEE 16th Intl. Conf. Comput. Vis. (ICCV), 2013, pp. 2976–2983.

[18] H. Jiang, J. Wang, Z. Yuan, Y. Wu, N. Zheng, and S. Li, "Salient object detection: A discriminative regional feature integration approach," in IEEE 26th Conf. Comput. Vis. Pattern Recognit. (CVPR), 2013, pp. 2083–2090.

[19] J. P. Papa, A. X. Falcão, and C. T. Suzuki, "Supervised pattern classification based on optimum-path forest," Int. J. Imaging Syst. Technol., vol. 19, no. 2, pp. 120–131, 2009.

[20] T. Liu, Z. Yuan, J. Sun, J. Wang, N. Zheng, X. Tang, and H.-Y. Shum, "Learning to detect a salient object," IEEE Trans. Pattern Anal. Mach. Intell., vol. 33, no. 2, pp. 353–367, 2011.

[21] L. Mansilla and P. Miranda, "Oriented image foresting transform segmentation: Connectivity constraints with adjustable width," in Proc. 29th Conf. Graphics Pattern Images (SIBGRAPI). IEEE, 2016, pp. 289–296.

[22] P. Neubert and P. Protzel, "Superpixel benchmark and comparison," in Proc. Forum Bildverarbeitung, vol. 6, 2012, pp. 1–12.